Theoretical studies of phosphorene as a drug delivery nanocarrier for fluorouracil

Razieh Esfandiarpour*,a, Farideh Badalkhani-Khamseh*,a, Nasser L. Hadipour*,a

aDepartment of Physical Chemistry, Faculty of Sciences, Tarbiat Modares University, Tehran, Iran

razieh_esf@yahoo.com

f.badalkhani@modares.ac.ir

hadipour@modares.ac.ir

Table S1. Calculated Fukui indices for the electrophilic (f_k^-), nucleophilic (f_k^+), and radical attack (f_k^0), susceptibility of FLU atoms.

Atoms	(f_k^-)	(f_k^+)	(f_k^0)
C1	0.0008	0.6515	0.3261
N2	0.0004	0.0091	0.0047
C2	0.0031	0.0001	0.0016
C3	0.0092	0.0001	0.0047
C4	0.0115	0.0001	0.0058
N1	0.0062	0.0089	0.0076
H1	0	0	0
H2	0	0	0
H3	0	0	0
O1	0	0.3301	0.1651
O2	0.9686	0	0.4843
F	0.0002	0	0.0001

Table S2. The calculated adsorption energies (E_{ads}) in kcal.mol^{-1} and total charge transfer (Q_T) in $|e|$ occurred upon adsorption of FLU molecule on top of pristine PNS, its carbon doped (CPNS), and its nitrogen doped (NPNS) analogues in gas phase. The E_{ads} values are reported considering the BSSE correction terms.

Structure	PNS		CPNS		NPNS	
	E_{ads}	Q_T	E_{ads}	Q_T	E_{ads}	Q_T
PNS-F	-17.54	0.037	-16.93	0.037	-17.07	0.031
PNS-N1	-18.51	0.037	-17.62	0.032	-18.20	0.032
PNS-N2	-17.04	0.030	-18.87	0.038	-19.03	0.039
PNS-O1	-17.04	0.029	-16.79	0.034	-16.86	0.037
PNS-O2	-18.64	0.038	-16.94	0.035	-17.23	0.038
PNS-h	-18.07	0.04	-17.30	0.033	-17.42	0.034

Table S3. All second-order perturbation energy ($E^{(2)}$ in kcal.mol^{-1}) for the most stable complexes formed between the FLU molecule and pristine PNS, CPNS, and NPNS.

		Nanosheet → Drug			Drug → Nanosheet	
	Donor	**Acceptor**	$E^{(2)}$	**Donor**	**Acceptor**	$E^{(2)}$
			Gas Phase			
PNS-O2	LP (1) P47	BD*(2) C1-O1	0.85	BD*(2) C1-O1	BD*(1) P47-P112	5.76
	BD (1) P48-P113	RY*(2) O2	0.52	BD*(2) C4-O2	BD*(1) P48-P113	4.32
	LP (1) P13	BD*(2) C2-C3	0.4	LP (1) O2	BD*(1) P48-P113	2.27
	BD (1) P17-P47	RY*(4) C1	0.34	BD (2) C1-O1	BD*(1) P17-P81	1.28
CPNS-N2	LP (1) P13	BD*(2) C1-O1	0.52	BD*(2) C4-O2	BD*(1) P12-P75	1.65
	BD (1) P13-P76	RY*(4) C1	0.23	LP (1) O2	BD*(1) P12-P75	0.78
	LP (1) P13	BD*(2) C4-O2	0.21	LP (1) O1	BD*(1) P18-P81	0.63
	LP (1) P43	BD*(2) C2-C3	0.21	BD (2) C1-O1	BD*(1) P18-P81	0.56
	BD (1) P43-P107	RY*(1) C2	0.16	LP (1) O2	BD*(1) P47-P111	0.35
NPNS-N2	LP (1) P13	BD*(2) C1-O1	1.11	BD*(2) C1-O1	BD*(1) P13-P76	6.99
	BD (1) P13-P76	RY*(4) C1	0.49	BD*(2) C4-O2	BD*(1) P12-P75	3.1
	LP (1) P43	BD*(2) C2-C3	0.48	LP (1) O2	BD*(1) P12-P75	1.45
	BD (1) P18-P81	RY*(1) C1	0.41	LP (1) O1	BD*(1) P18-P81	1.42
	BD (1) P43-P107	RY*(1) C2	0.38	BD (2) C1-O1	BD*(1) P18-P81	1.39
			Aqueous Phase			
PNS-O2	LP (1) P47	BD*(2) C1-O1	0.79	BD*(2) C1-O1	BD*(1) P 47-P112	4.97
	BD (1) P48-P 113	RY*(2) O2	0.46	BD*(2) C4-O2	BD*(1) P 48-P113	3.73
	LP (1) P13	BD*(2) C2-C3	0.42	LP (1) O2	BD*(1) P 48-P113	2.07
	BD (1) P17-P47	RY*(4) C1	0.36	BD (2) C1-O1	BD*(1) P17-P81	1.11
	BD (1) P47-P112	RY*(4) C1	0.33	BD (2) C4-O2	BD*(1) P48-P113	1.01
CPNS-N2	LP (1) P13	BD*(2) C1-O1	0.43	BD*(2) C4-O2	BD*(1) P12-P75	1.19
	BD (1) P 13-P76	RY*(4) C1	0.23	LP (1) O2	BD*(1) P12-P75	0.73
	LP (1) P13	BD*(2) C4-O2	0.16	BD (2) C1-O1	BD*(1) P18-P81	0.55
	LP (1) P43	BD*(2) C2-C3	0.15	LP (1) O1	BD*(1) P18-P81	0.5
	BD (1) P18-P81	RY*(1) C1	0.14	LP (1) N2	BD*(1) P13-P76	0.32
NPNS-N2	LP (1) P13	BD*(2) C1-O1	1.01	BD*(2) C1-O1	BD*(1) P13-P76	5.66
	BD (1) P 13-P 76	RY*(4) C1	0.52	BD*(2) C4-O2	BD*(1) P12-P75	2.26
	BD (1) P18-P81	RY*(1) C1	0.38	LP (1) O2	BD*(1) P12-P75	1.38
	LP (1) P43	BD*(2) C2-C3	0.32	BD (2) C1-O1	BD*(1) P18-P81	1.27
	LP (1) P13	BD*(2) C4-O2	0.26	LP (1) O1	BD*(1) P18-P81	1.13

Table S4. Quantum chemistry reactivity parameters (in eV) including: E_{HOMO}, E_{LUMO}, and their associated energy gap (E_g), ionization potential (I), electron affinity (A), electronegativity (χ), chemical hardness (η), and electronic chemical potential (μ) for nanosheets and their most stable complexes.

System	Phase	E_{HOMO} = -I	E_{LUMO} = -A	E_g	χ	η	μ
PNS		-6.8	-2.6	4.1	4.7	2.1	-4.7
PNS-F		-6.8	-2.6	4.2	4.7	2.1	-4.7
PNS-N1		-6.8	2.6	9.3	2.1	4.7	-2.1
PNS-N2		-6.7	-2.6	4.2	4.7	2.1	-4.7
PNS-O1		-6.8	-2.6	4.2	4.7	2.1	-4.7
PNS-O2		-6.8	-2.6	4.2	4.7	2.1	-4.7
PNS-*h*		-6.7	-2.6	4.2	4.7	2.1	-4.7
CPNS		-6.6	-2.5	4.1	4.6	2.0	-4.6
CPNS-F		-6.6	-2.5	4.1	4.6	2.0	-4.6
CPNS-N1		-6.6	-2.5	4.1	4.5	2.0	-4.5
CPNS-N2	Gas	-6.6	-2.5	4.1	4.6	2.1	-4.6
CPNS-O1		-6.6	-2.5	4.1	4.6	2.0	-4.6
CPNS-O2		-6.6	-2.5	4.1	4.6	2.0	-4.6
CPNS-*h*		-6.6	-2.5	4.1	4.5	2.0	-4.5
NPNS		-6.8	-2.6	4.2	4.7	2.1	-4.7
NPNS-F		-6.7	-2.6	4.2	4.7	2.1	-4.7
NPNS-N1		-6.8	-2.6	4.2	4.7	2.1	-4.7
NPNS-N2		-6.8	-2.6	4.2	4.7	2.1	-4.7
NPNS-O1		-6.8	-2.6	4.2	4.7	2.1	-4.7
NPNS-O2		-6.7	-2.5	4.2	4.6	2.1	-4.6
NPNS-*h*		-6.7	-2.5	4.2	4.6	2.1	-4.6
PNS		-8.1	-0.1	7.9	4.1	4.0	-4.1
PNS-O2		-6.8	-2.6	4.2	4.7	2.1	-4.7
CPNS	Aqueous	-6.8	-2.6	4.2	4.7	2.1	-4.7
CPNS-N2		-6.7	-2.5	4.1	4.6	2.1	-4.6
NPNS		-6.6	-2.5	4.1	4.6	2.1	-4.6
NPNS-N2		-6.8	-2.6	4.2	4.7	2.1	-4.7

Force Field Development

To create the parameter and coordinate files for PNS and FLU molecules, we used the GAMESS software at the B3LYP level of theory and 6-31G(d) basis set for structural optimization, and charge distributions were obtained from Mulliken analysis. Then, the Antechamber tools with "LEaP" was used to generate "general AMBER force field (GAFF)" topology and coordinate files for the prescription PNS and drug FLU. This force field has been specifically designed to cover most pharmaceutical molecules and is compatible with the traditional AMBER force fields in such a way that the two can be mixed during a molecular dynamics (MD) simulation. Like the traditional AMBER force fields, GAFF uses a simple harmonic function form for bonds and angles but unlike the traditional protein and DNA orientated AMBER force fields the atom types used in GAFF are much more general such that they cover most of the organic chemical space. The current implementation of the GAFF force field consists of basic atom types and special atom types. The charge method used here is HF/6-31G* RESP (restrained electrostatic potential). Moreover, since GAFF is totally compatible with the AMBER macromolecular force fields it should prove to be a useful molecular mechanical tool for rational drug design. Especially in binding free energy calculations and molecular docking studies. Using the utility "parmchk", we find that there is no missing bond, angle, or dihedral in the parameter file. Finally, we used the ACPYPE tool to convert the Antechamber output files to topology and coordinates files that are compatible with GROMACS software. To validate the partial atomic charges obtained using the RESP method, we compared them with those of regular uracil in CHARMM36m (Table S7), which are highly optimized and reliable as a reference for biomolecules.

Table S5. The force field nonbonded (σ and ε) parameters of PNS and FLU molecule.

Atom Type	σ	ε
PX	3.33E-01	1.67E+00
f	3.12E-01	2.55E-01
o	2.96E-01	8.79E-01
n	3.25E-01	7.11E-01
c	3.40E-01	3.60E-01
cc	3.40E-01	3.60E-01
cd	3.40E-01	3.60E-01
hn	1.07E-01	6.57E-02
h4	2.51E-01	6.28E-02
HW	0.00E+00	0.00E+00
OW	3.15E-01	6.36E-01
Cl	4.40E-01	4.18E-01
Na	3.33E-01	1.16E-02

Table S6. Atom type and assigned RESP charges for FLU molecule.

Atom Type	Atom No.	Charge
f	1	-0.17982
o	2	-0.5261
o	3	-0.55826
n	4	-0.42125
n	5	-0.34661
c	6	0.579787
c	7	0.589064
cc	8	0.128163
cd	9	-0.15826
hn	10	0.327092
hn	11	0.338407
h4	12	0.227787
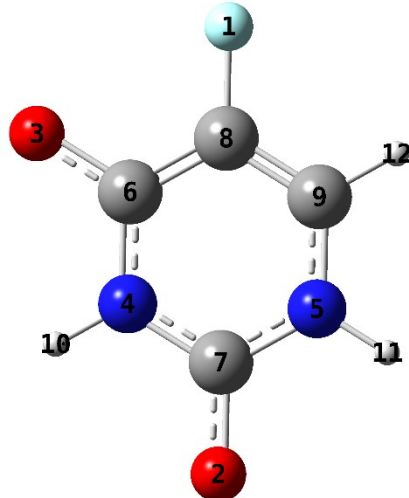
Table S7. Force Field parameters for uracil molecule obtained from GAFF and CHARMM36m force fields.

Atom	Atom Type	AMBER			CHARMM36m		
		Charge	σ	ε	Charge	σ	ε
C1	c	0.516	0.340	0.360	0.321	0.339	0.418
N1	n	-0.268	0.325	0.711	-0.395	0.330	0.837
C2	cc	-0.102	0.340	0.360	0.097	0.339	0.377
C3	cd	-0.308	0.340	0.360	-0.257	0.339	0.377
C4	c	0.572	0.340	0.360	0.403	0.339	0.418
N2	n	-0.339	0.325	0.711	-0.251	0.330	0.837
H1	h4	0.216	0.251	0.063	0.182	0.196	0.192
H2	hn	0.306	0.107	0.066	0.357	0.040	0.192
H3	hn	0.315	0.107	0.066	0.331	0.040	0.192
O1	o	-0.544	0.296	0.879	-0.433	0.303	0.502
O2	o	-0.542	0.296	0.879	-0.482	0.303	0.502
H4	ha	0.177	0.260	0.063	0.127	0.196	0.192
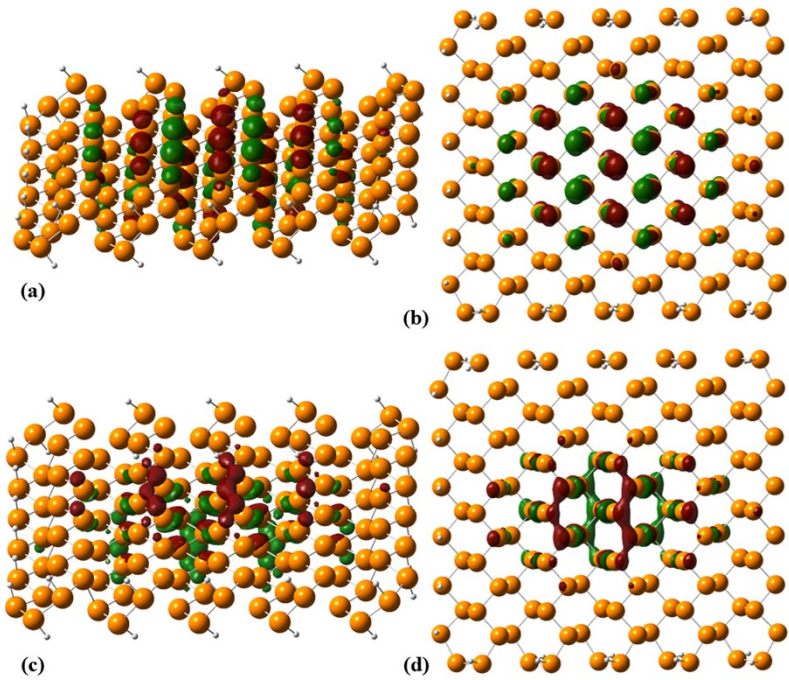
**Figure S1.** Side and top view of HOMO ((a) and (b)) and LUMO ((c) and (d)) profiles of PNS.
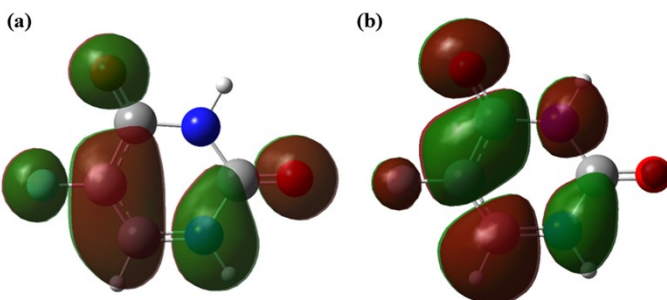
Figure S2. The (a) HOMO and (b) LUMO profiles of FLU molecule.
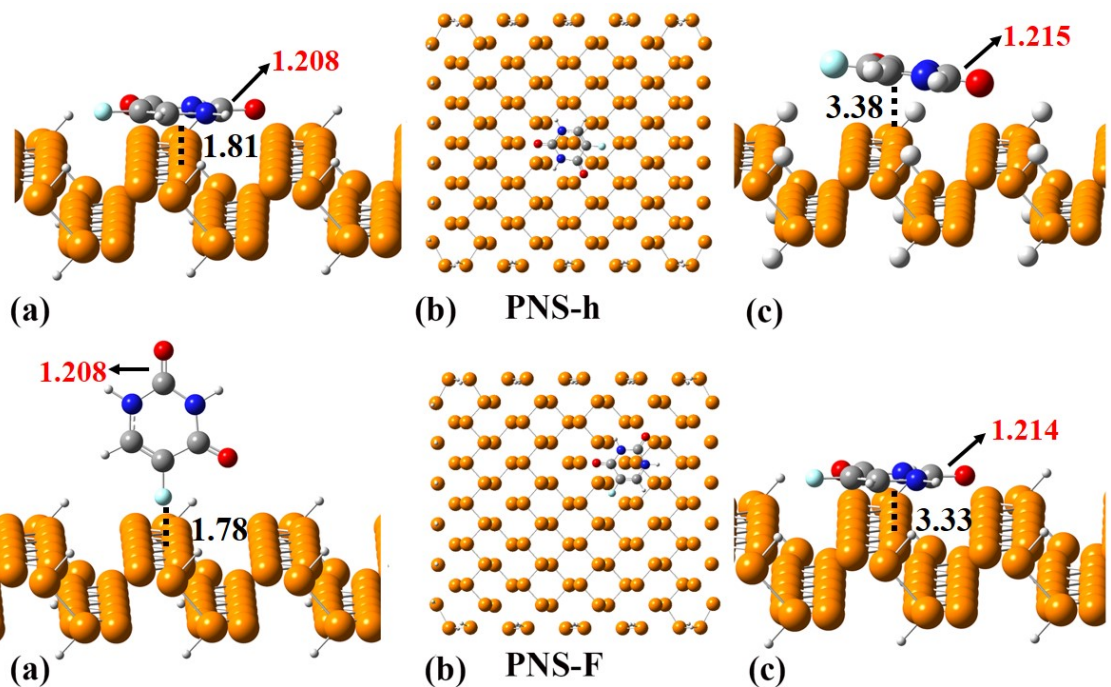
Figure S3. (a) Initial, (b) and (c) equilibrated structures of PNS-*h* and PNS-F calculated at M06-2X/6-31G(d,p).
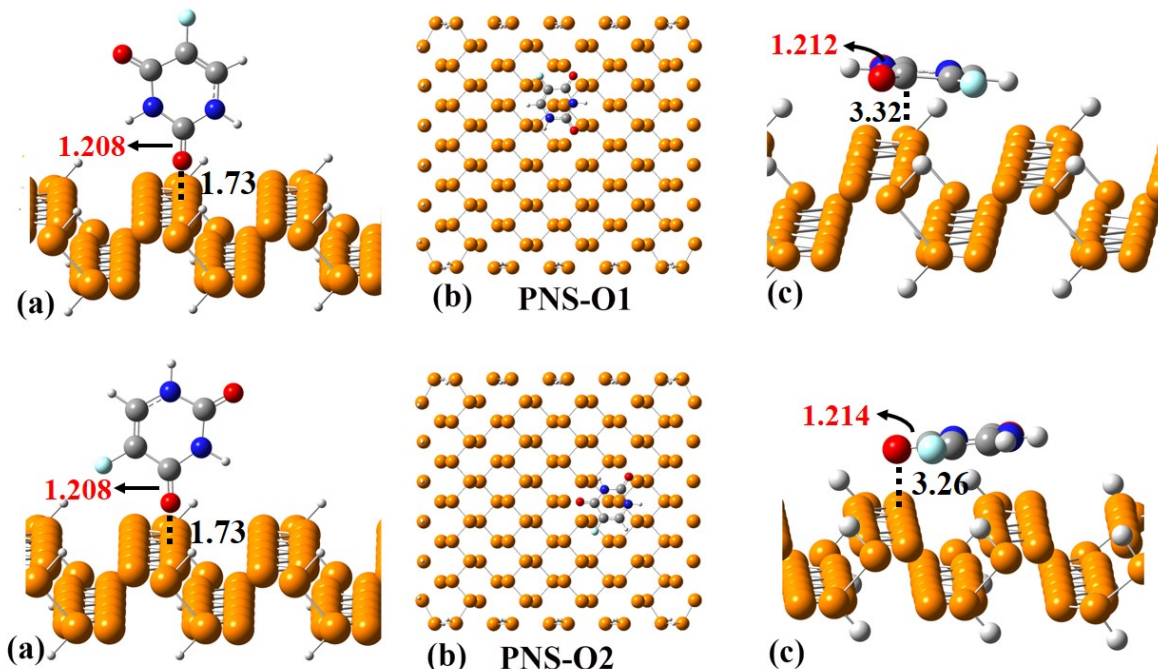
Figure S4. (a) Initial, (b) and (c) equilibrated structures of PNS-O1 and PNS-O2 calculated at M06-2X/6-31G(d,p).
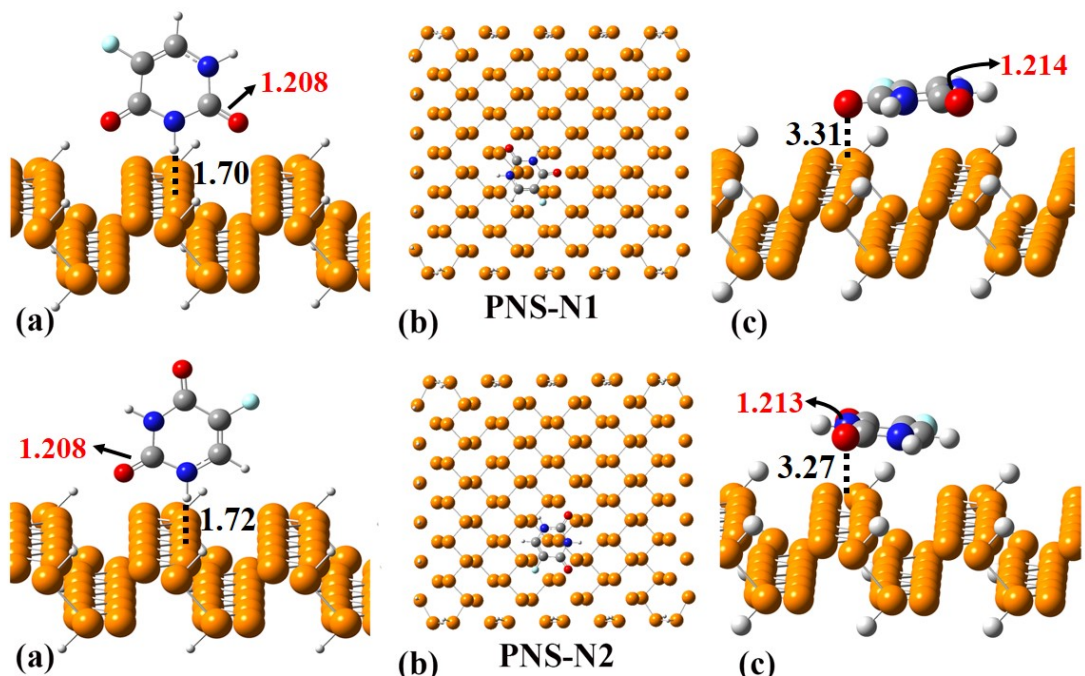
Figure S5. (a) Initial, (b) and (c) equilibrated structures of PNS-N1 and PNS-N2 calculated at M06-2X/6-31G(d,p).
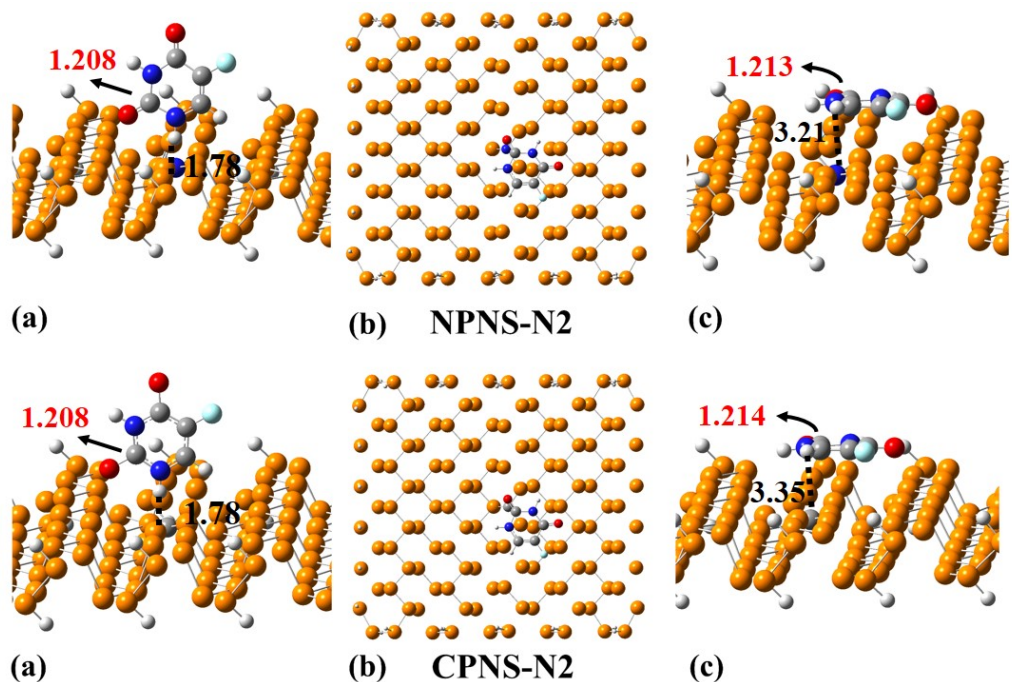
Figure S6. (a) Initial, (b) and (c) equilibrated structure of NPNS-N2 and CPNS-N2 calculated at M06-2X/6-31G(d,p).
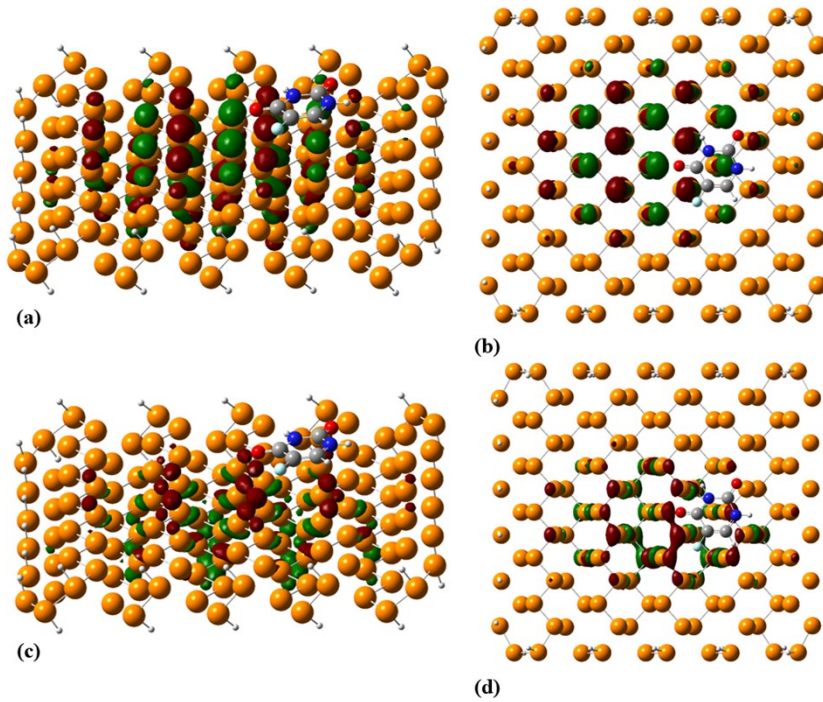
Figure S7. Side and top view of HOMO ((a) and (b)) and LUMO ((c) and (d)) profiles of PNS-O2.
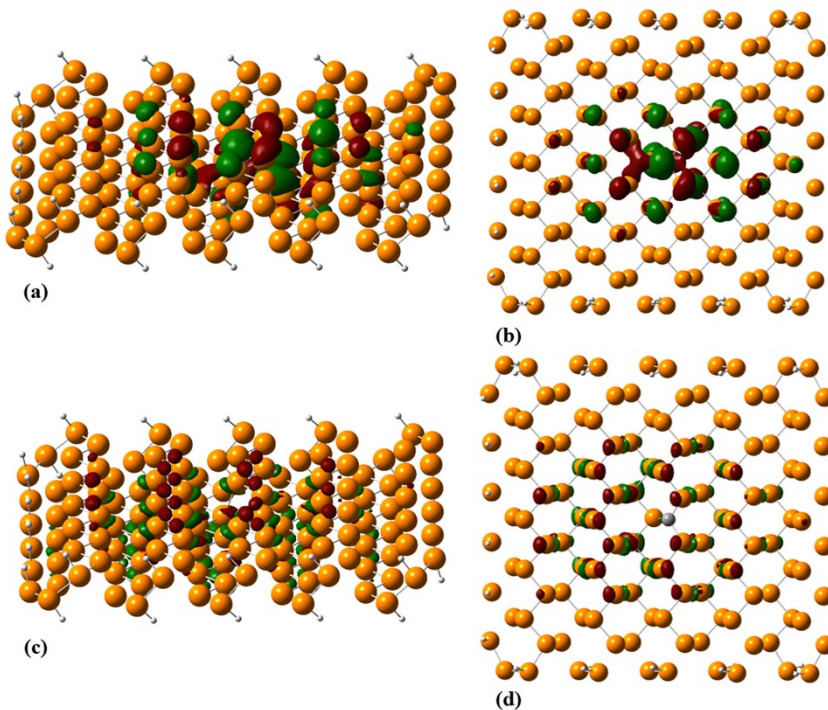
Figure S8. Side and top view of HOMO ((a) and (b)) and LUMO ((c) and (d)) profiles of CPNS.
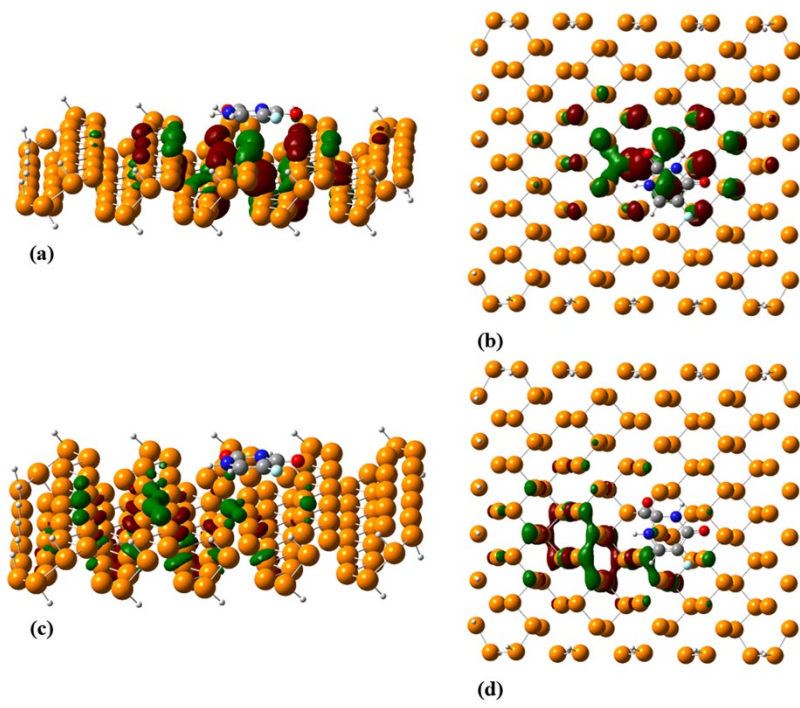
Figure S9. Side and top view of HOMO ((a) and (b)) and LUMO ((c) and (d)) profiles of CPNS-N2.
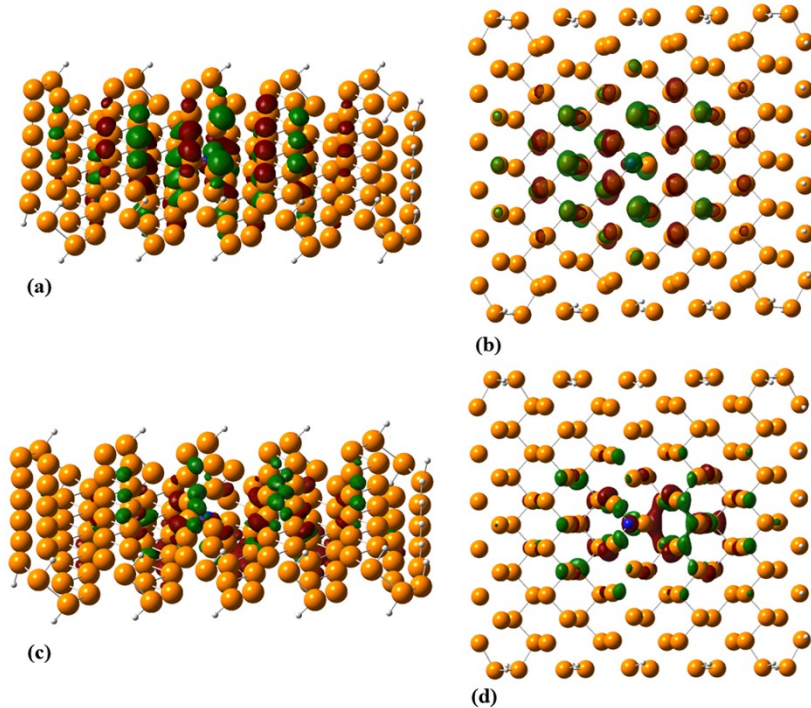
Figure S10. Side and top view of HOMO ((a) and (b)) and LUMO ((c) and (d)) profiles of NPNS.
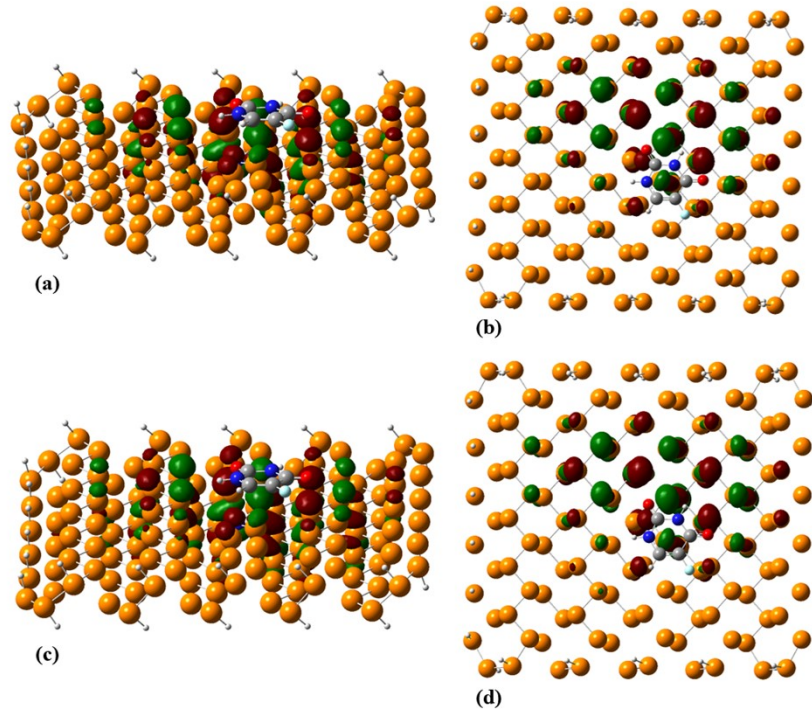
Figure S11. Side and top view of HOMO ((a) and (b)) and LUMO ((c) and (d)) profiles of NPNS-N2.
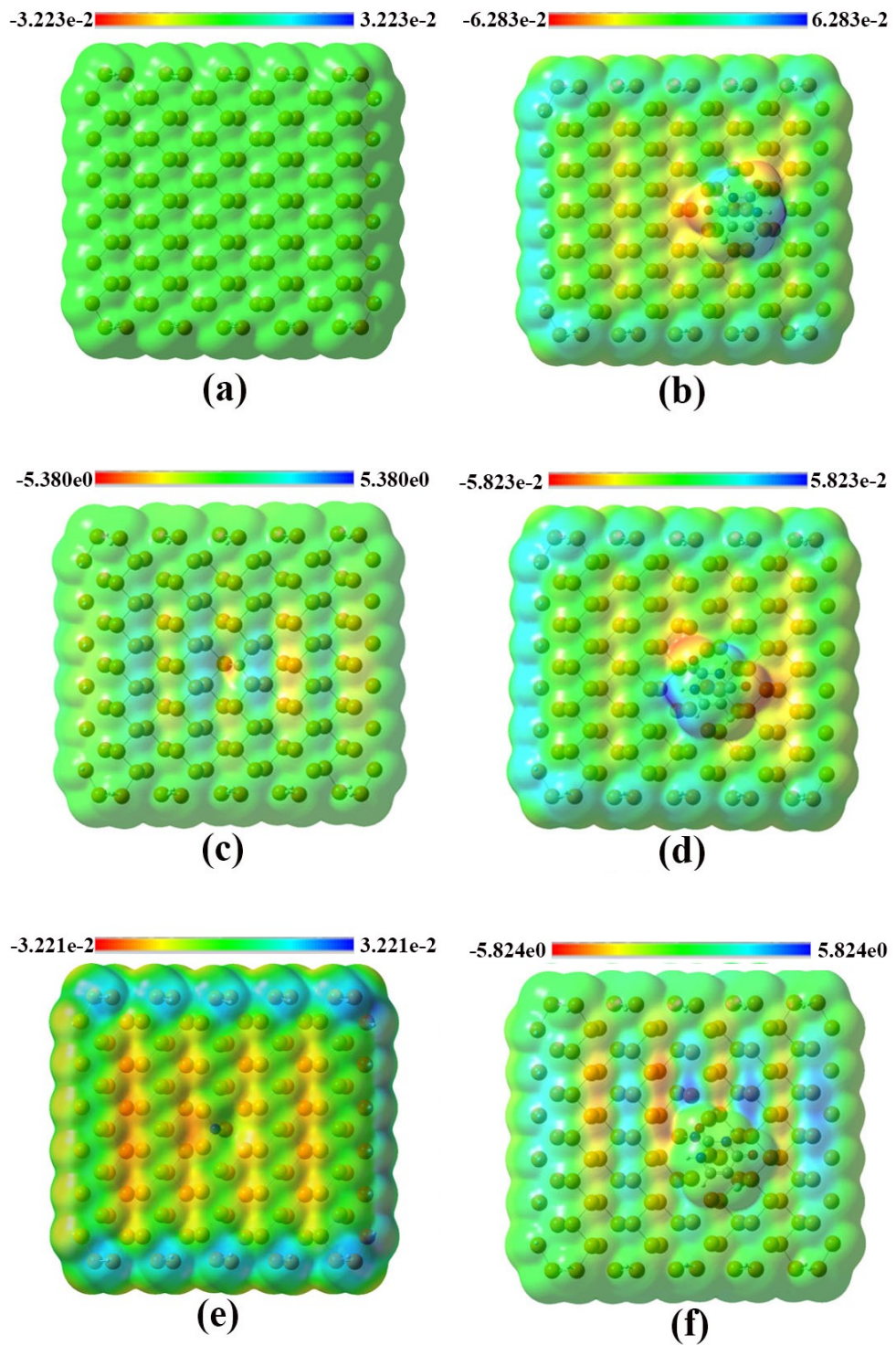
Figure S12. MEP plot of (a) PNS, (b) PNS-O2, (c) CPNS, (d) CPNS-N2, (e) NPNS and (f) NPNS-N2 calculated at M06-2X/6-31G(d,p).
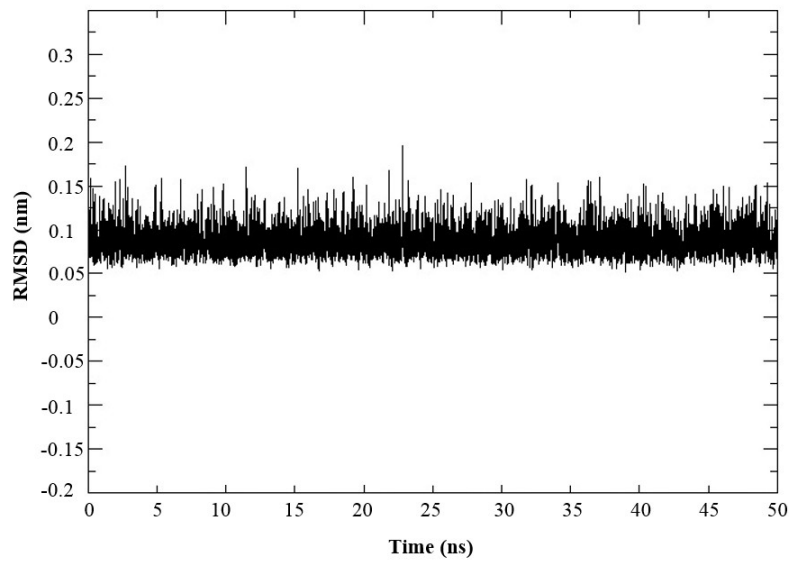
Figure S13. Atom-positional RMSD of the PNS molecule during the MD simulations.
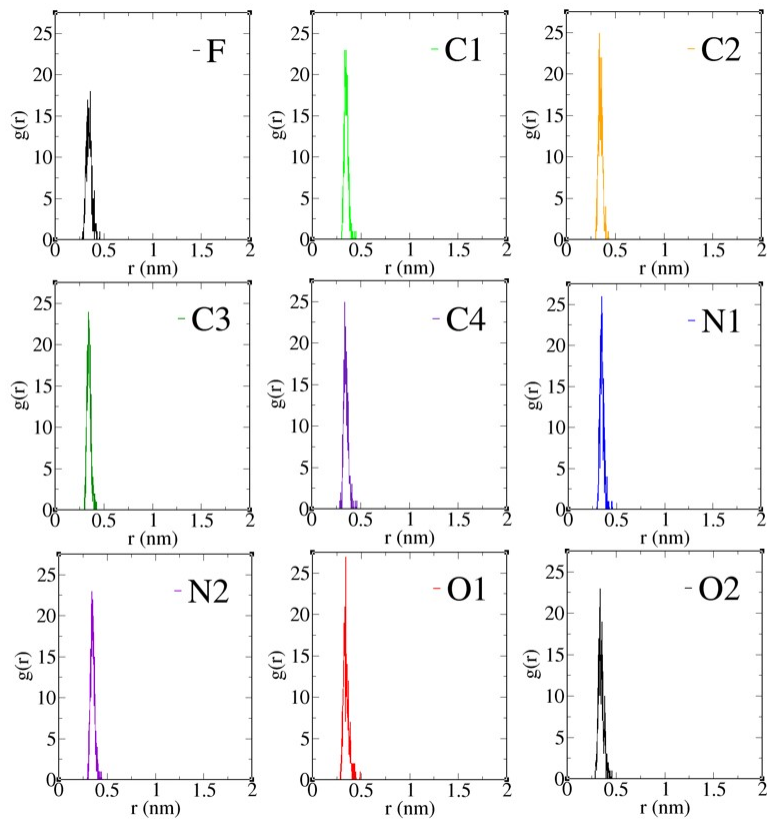
Figure S14. Radial pair distribution functions (RDF) of the FLU atoms to the PNS molecule at 310 K.
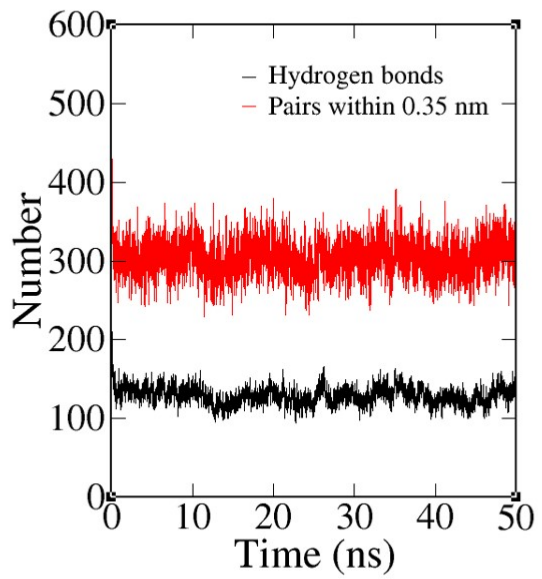
Figure S15. The number of hydrogen bonds formed between FLU drug molecules and water molecules in PNS-60FLU system.
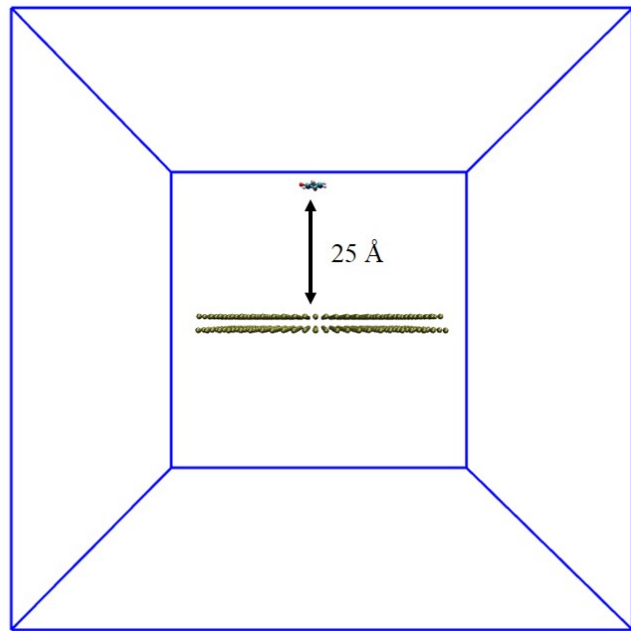
Figure S16. Geometry of PNS-FLU system at the beginning of MD simulations.

(a)   (b)
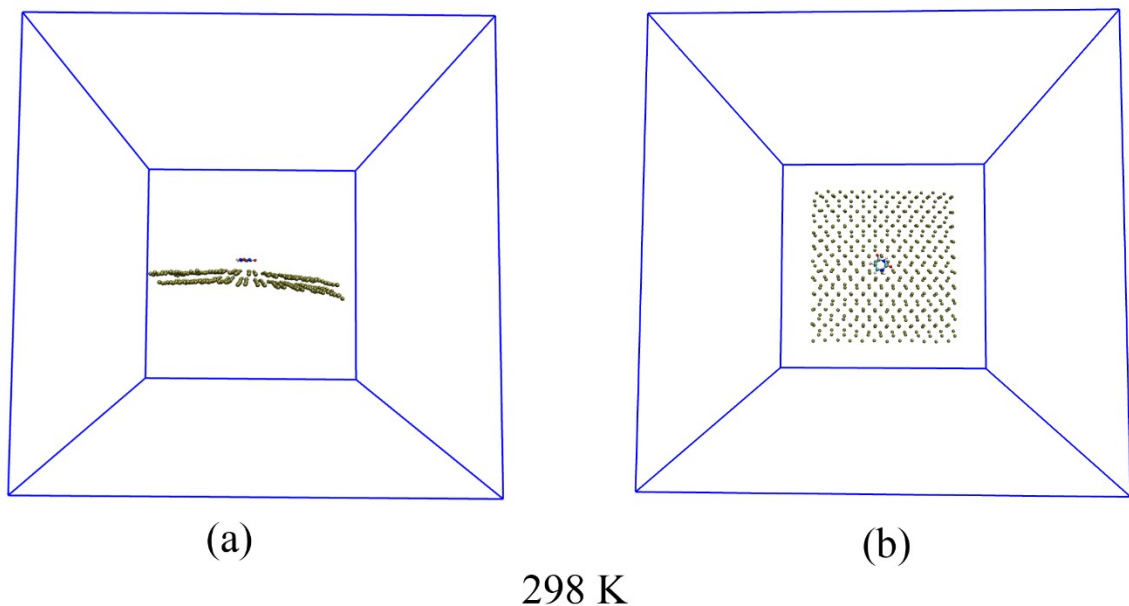
298 K

Figure S17. (a) Side and (b) top view of equilibrated geometry of PNS-FLU at 298 K.

(a)   (b)
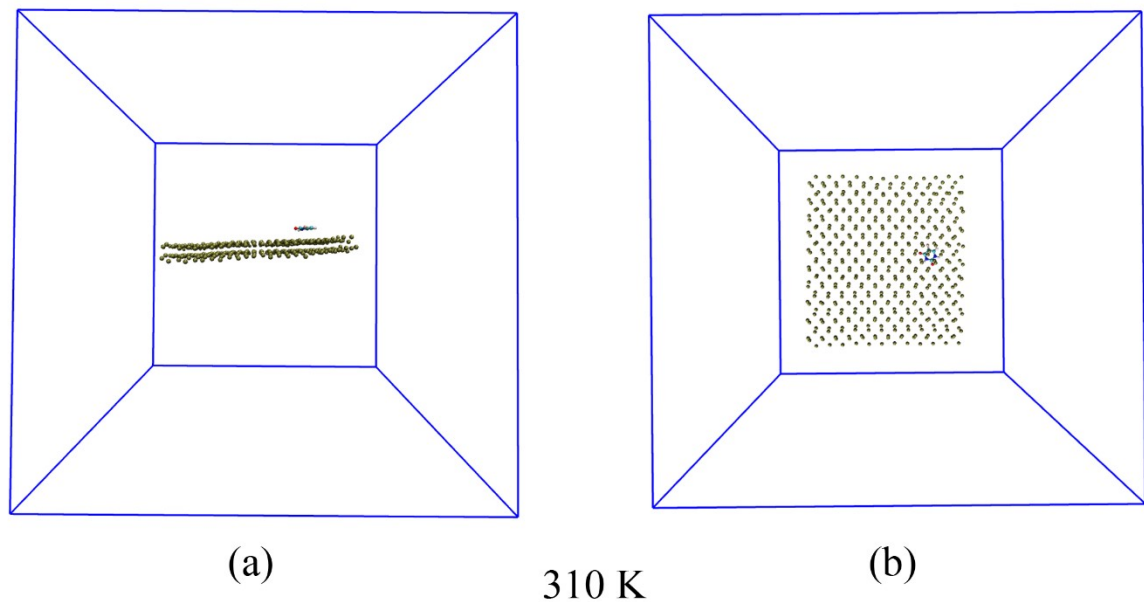
310 K

Figure S18. (a) Side and (b) top view of equilibrated geometry of PNS-FLU at 310 K.

(a)

326 K

(b)
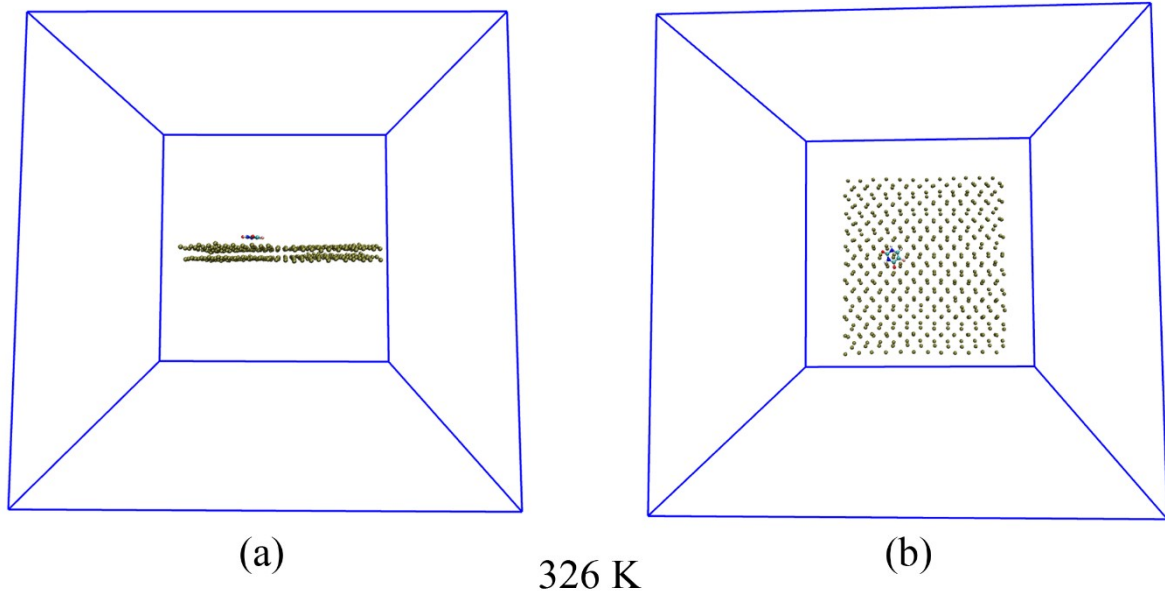
Figure S19. (a) Side and (b) top view of equilibrated geometry of PNS-FLU at 326 K.
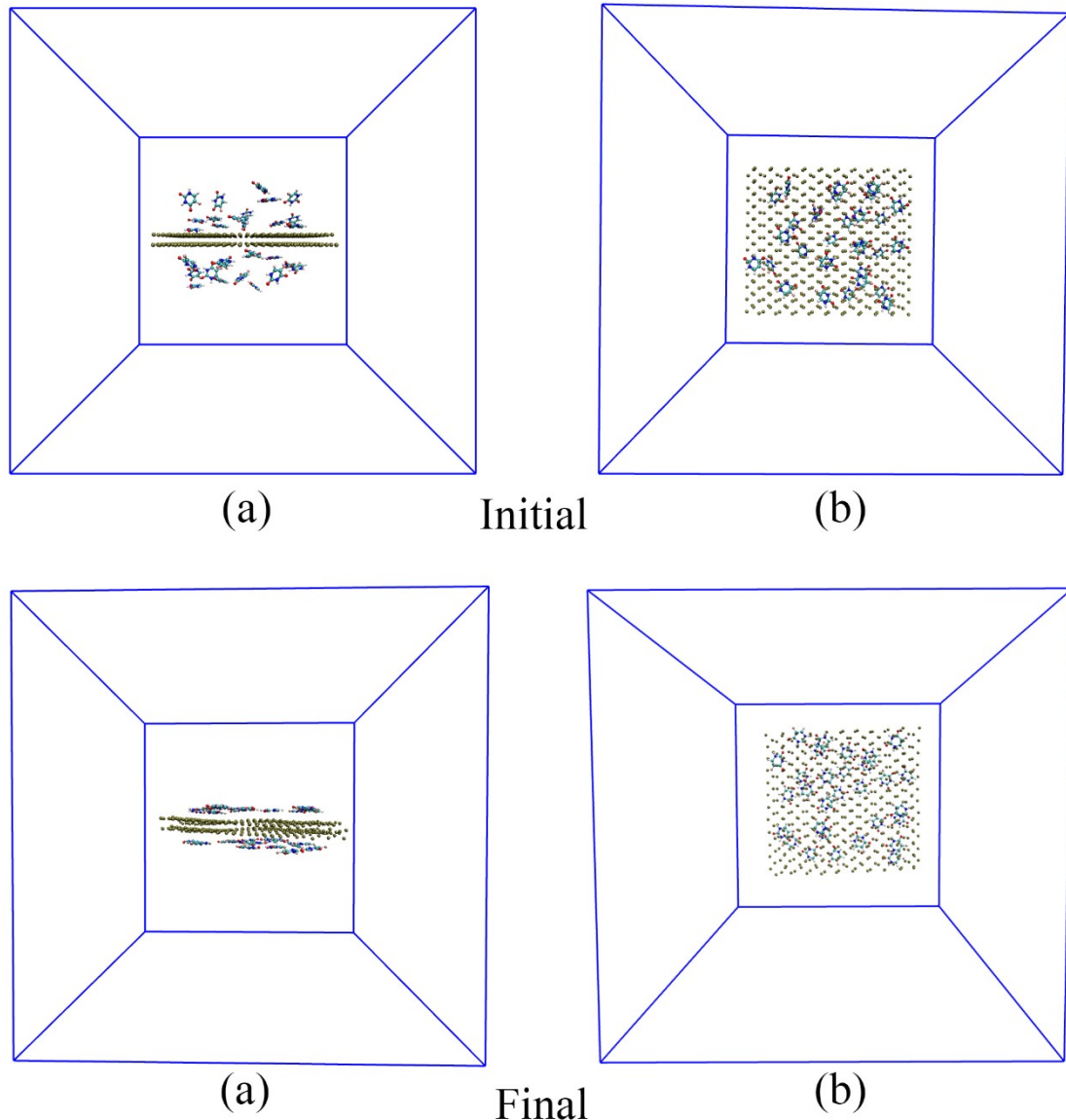
Figure S20. (a) Side and (b) top view of equilibrated geometry of PNS-30FLU at 310 K.
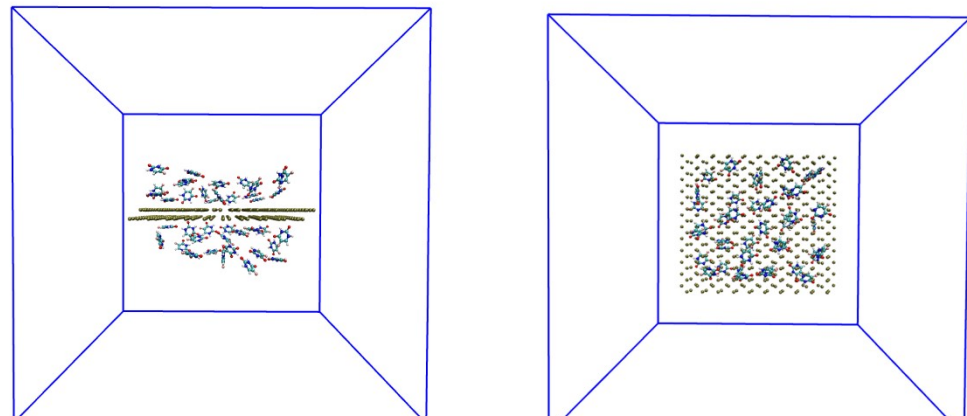
(a)   Initial   (b)
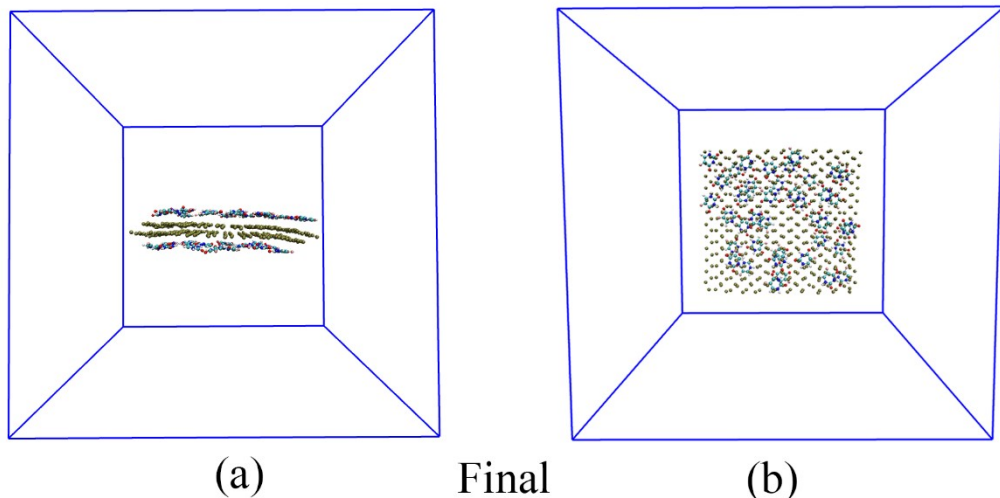
(a)   Final   (b)

Figure S21. (a) Side and (b) top view of equilibrated geometry of PNS-40FLU at 310 K.
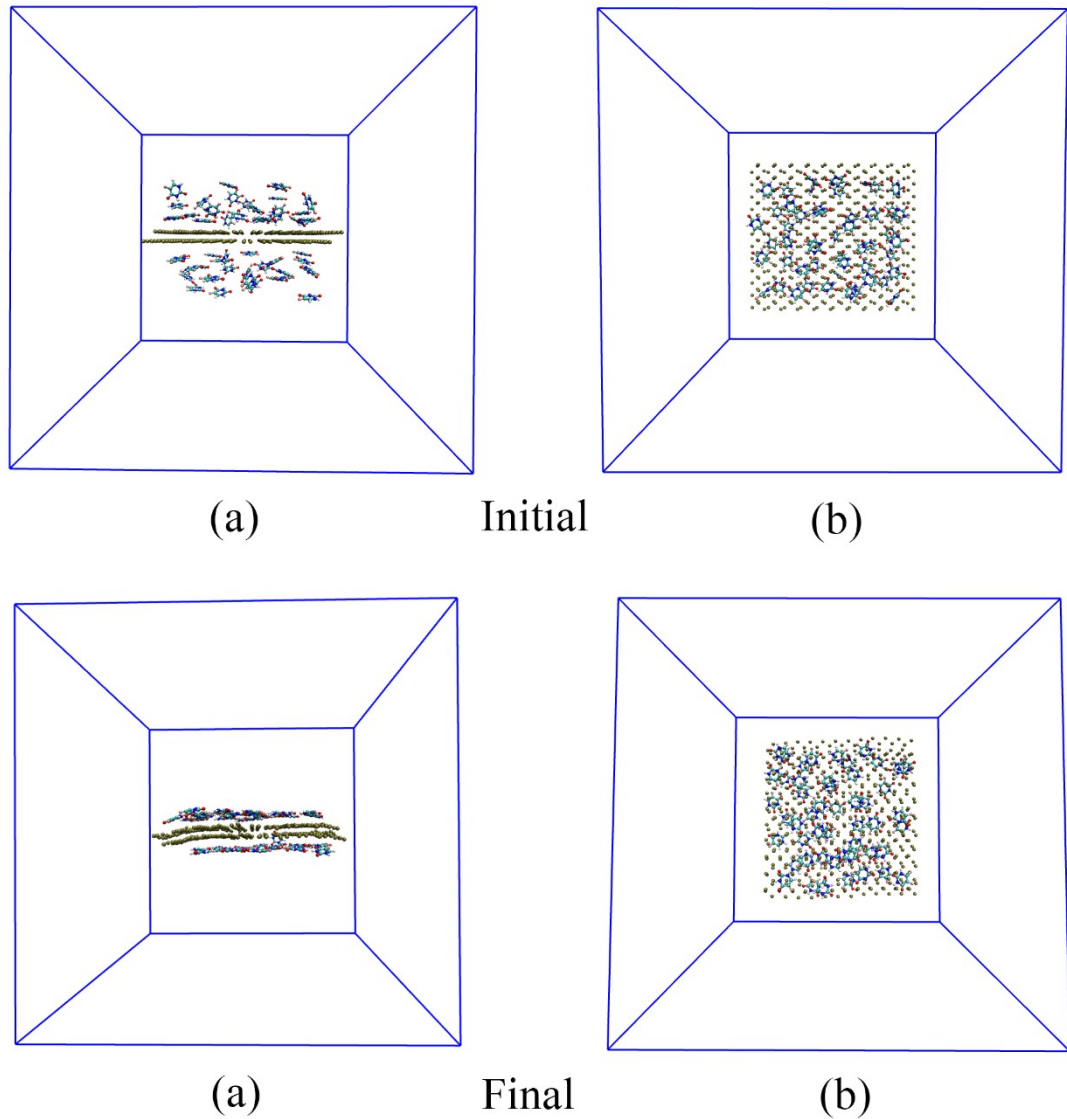
(a)   Initial   (b)

(a)   Final   (b)

Figure S22. (a) Side and (b) top view of equilibrated geometry of PNS-50FLU at 310 K.
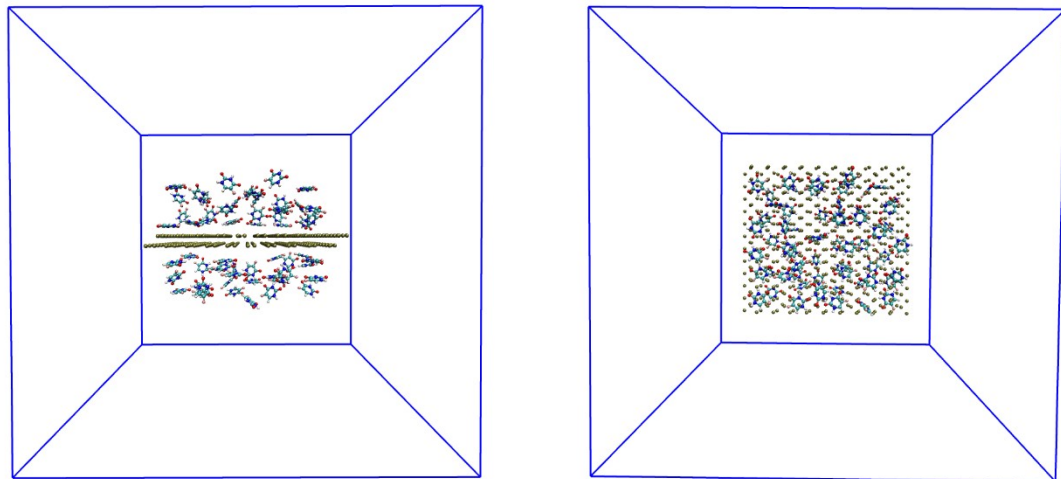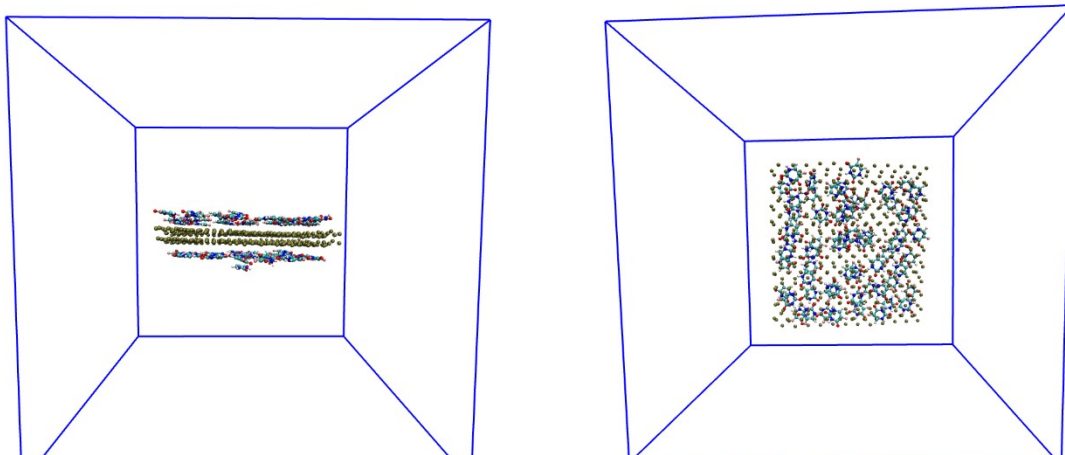
Figure S23. (a) Side and (b) top view of equilibrated geometry of PNS-60FLU at 310 K.

(a)   Initial   (b)

(a)   Final   (b)
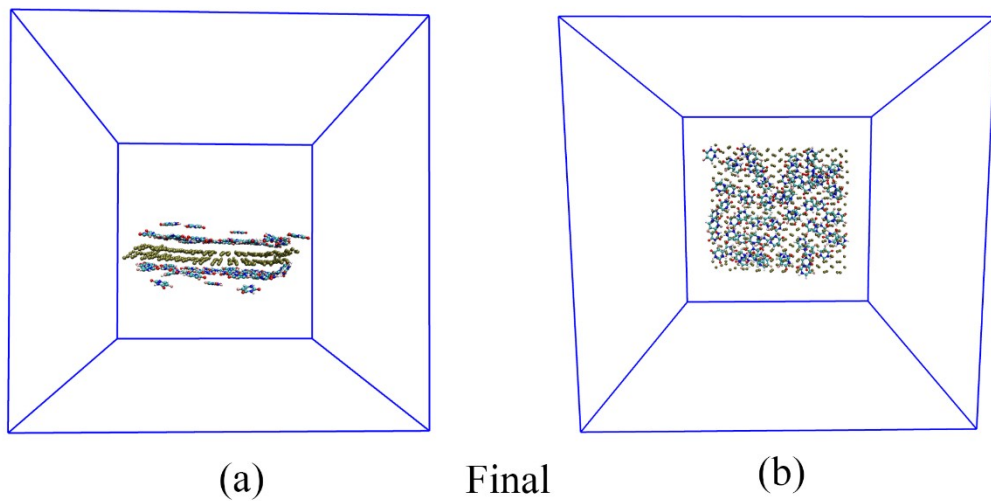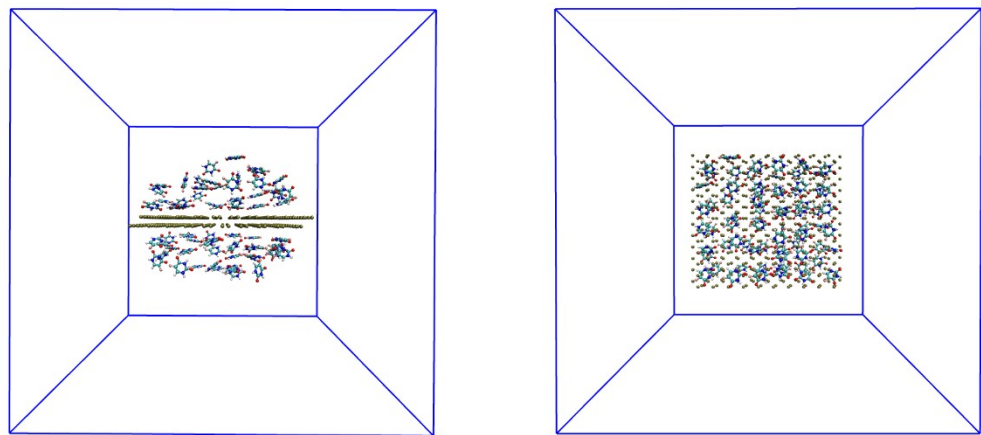
Figure S24. (a) Side and (b) top view of equilibrated geometry of PNS-70FLU at 310 K.

(a)　　　　　Initil　　　　　(b)

(a)　　　　　Final　　　　　(b)
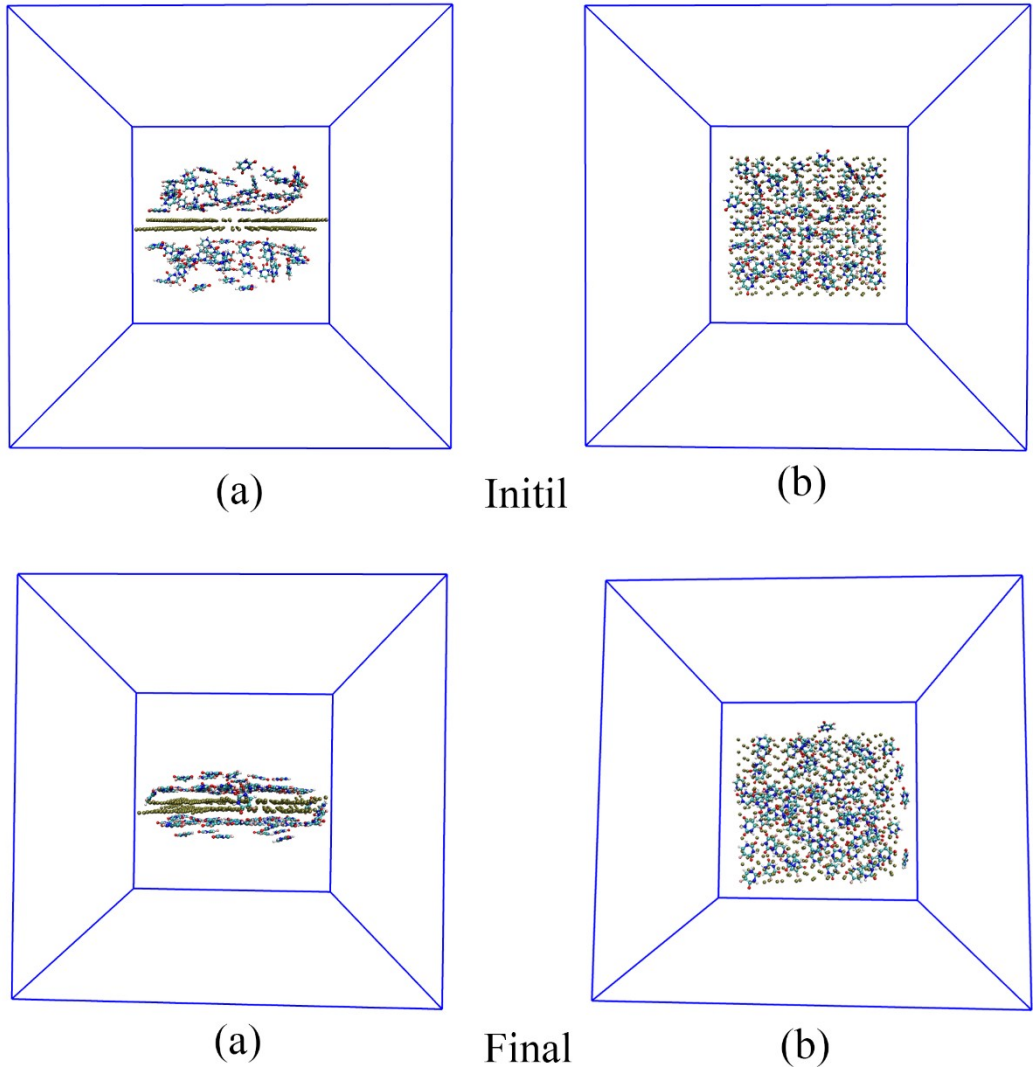
Figure S25. (a) Side and (b) top view of equilibrated geometry of PNS-80FLU at 310 K.